Catalytic Mechanism of CMP:2-Keto-3-deoxy-*manno*-octonic Acid Synthetase As Derived from Complexes with Reaction Educt and Product[†,‡]

Stefan Jelakovic and Georg E. Schulz*

Institut für Organische Chemie und Biochemie, Albert-Ludwigs-Universität, Albertstrasse 21, Freiburg im Breisgau, Germany 79104

Received October 9, 2001; Revised Manuscript Received November 29, 2001

ABSTRACT: The activation of the sugar 2-keto-3-deoxy-*manno*-octonic acid (Kdo) is catalyzed by CMP-Kdo synthetase (EC 2.7.7.38) and results in a monophosphate diester with CMP. The enzyme is a pharmaceutical target because CMP-Kdo is required for the biosynthesis of lipopolysaccharides that are vital for Gram-negative bacteria. We have established the structures of an enzyme complex with the educt CTP and of a complex with the product CMP-Kdo by X-ray diffraction analyses at 100 K, both at 2.6 Å resolution. The N-terminal domains of the dimeric enzyme bind CTP in a peculiar nucleotide-binding fold with the β- and γ-phosphates located at the so-called "PP-loop", whereas the C-terminal domains participate in Kdo binding and in the dimer interface. The unstable nucleotide-sugar CMP-Kdo was produced in a crystal and stabilized by freezing to 100 K. Its formation is accompanied by an induced fit involving mainchain displacements in the 2 Å range. The observed binding conformations together with the amino acid conservation pattern during evolution and the putative location of the required Mg^{2+} ion suggest a reaction pathway. The enzyme is structurally homologous to the CMP-*N*-acetylneuraminic acid synthetases in all parts except for the dimer interface. Moreover, the chainfold and the substrate-binding positions resemble those of other enzymes processing nucleotide sugars.

The rapid spread of drug-resistant bacteria has renewed the interest in novel classes of antibiotics. An attractive target against Gram-negative bacteria is the outer membrane with its lipopolysaccharides (LPS).[1] LPS formation requires 2-keto-3-deoxy-*manno*-octonic acid (Kdo) which connects the lipid A moiety with the core oligosaccharides (*1*−*3*). Kdo is activated by CMP-Kdo synthetase (CKS), that catalyzes the formation of a monophosphate diester according to the reaction scheme shown in Figure 1 (*4*, *5*). The resulting nucleotide-sugar CMP-Kdo is the substrate of a series of transferases that incorporate Kdo into lipo- and capsular polysaccharides. CMP-Kdo formation is the rate-limiting step in lipopolysaccharide biosynthesis (*4*). Kdo and *N*-acetylneuraminic acid (NeuAc) (Figure 1) are unique in as far as their activated forms are nucleoside monophosphate diesters, rather than the more common nucleoside diphosphate diesters (*6*).

Two isozymes of CKS have been found in *Escherichia coli*. One of them participates in the biosynthesis of LPS and has been named L-CKS. The other isozyme was named "capsule-specific CKS" or K-CKS because it was detected in pathogenic strains where it is correlated with capsule expression (*7*, *8*). It shows 43% sequence identity with L-CKS and distinctly different enzyme kinetics (*9*, *10*). Some encapsulated *E. coli* strains cause extra-intestinal infections such as urinary tract and postoperative wound infections as well as sepsis and meningitis (*11*, *12*), indicating that the capsules are important virulence factors. Since Kdo is vital for Gram-negative bacteria and absent from mammalian cells, CKS is an attractive drug target (*13*). The chainfold of the unligated capsule-specific CKS from *E. coli* (*14*) and the refined atomic structures of the unligated CKS as well as of the CKS complexes with CMP, CDP, CTP, and with the product analogue CMP-NeuAc are known (*15*). All of them were determined at room temperature. Here we present two low-temperature structures of CKS complexes with the educt CTP and the product CMP-Kdo, establishing the active center and suggesting a detailed catalytic mechanism.

MATERIALS AND METHODS

Protein Purification, Crystallization, and Data Collection. The capsule-specific CKS from *E. coli* was cloned into the expression vector pUAKyI and expressed in *E. coli* as described earlier (*14*). The resulting enzyme was purified by ammonium sulfate precipitation followed by a Reactive Red affinity column (Sigma) and a Resource Q column (Pharmacia) as described (*14*). The yield was about 50 mg of pure protein per liter culture. The purified dimeric CKS with an M_r of 27028 per subunit was crystallized as described (*15*).

[†] The project was supported by the Deutsche Forschungsgemeinschaft under SFB-388.

[‡] The coordinates and structure factors are deposited in the Protein Data Bank under accession codes 1GQ9 and 1GQC.

* Corresponding author: Dr. Georg E. Schulz, Institut für Organische Chemie und Biochemie, Albertstr. 21, D-79104 Freiburg im Breisgau, Germany, Telephone: +49-761-203-6058, FAX: +49-761-203-6161, E-mail: schulz@bio.chemie.uni-freiburg.de.

[1] Abbreviations: CKS, CMP-Kdo synthetase (here generally the capsule-specific isoenzyme from *Escherichia coli*); CMP-NeuAc, cytidine 5′-monophospho 5-*N*-acetylneuraminic acid; CNS, CMP-NeuAc synthetase; Kdo, 2-keto-3-deoxy-*manno*-octonic acid; LPS, lipopolysaccharide; NeuAc, 5-*N*-acetylneuraminic acid (sialic acid).

10.1021/bi0119060 CCC: $22.00
Published on Web 01/04/2002

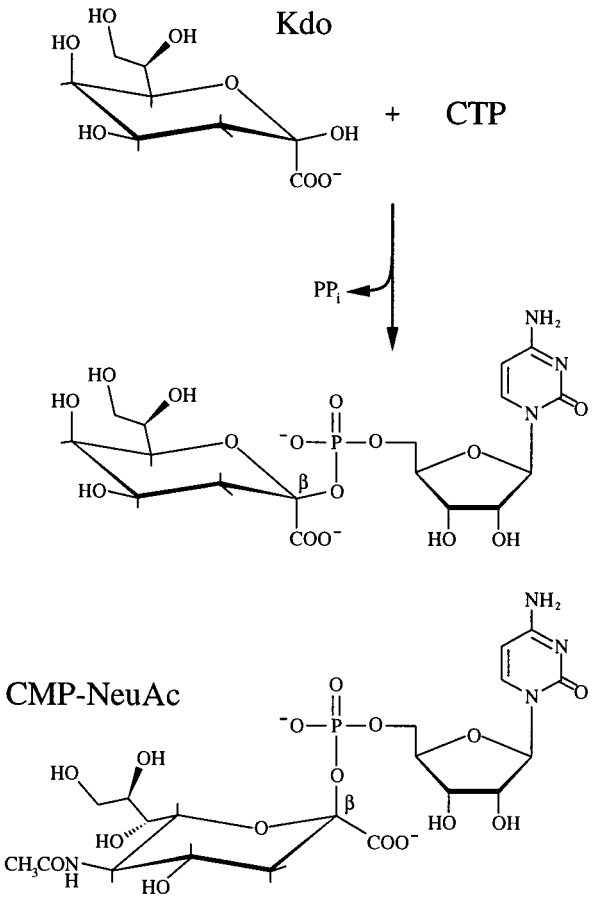

FIGURE 1: The reaction scheme of Kdo activation as catalyzed by CKS. Kdo favors the displayed $^5C_2$ chair conformation. The resulting monophosphate diester CMP-Kdo has a half-life of about 30 min under physiological conditions. The structure of CMP-NeuAc is given below for comparison.

For the CTP complex structure analysis we used a crystal of 300 × 120 × 40 μm^3 and soaked it for 25 min in 10 mM CTP, 1.3 mM $MgCl_2$, 75 mM Tris-HCl, pH 9.4, 12% PEG-20000, and 150 mM $Ca(OAc)_2$. After that, the crystal was transferred for about half a minute to 30% (v/v) glycerol, 70 mM Tris-HCl, pH 9.4, 11% PEG-20000, and 140 mM $Ca(OAc)_2$, quickly frozen to 100 K and used for data collection. The crystal diffracted to 2.4 Å resolution and belonged to space group $P2_1$ with a dimeric CKS molecule in the asymmetric unit and cell parameters $a = 45.7$ Å, $b = 132.3$ Å, $c = 47.9$ Å, $\beta = 102.4°$. It was isomorphous with the crystals of unligated CKS at room temperature ($a = 46.1$ Å, $b = 133.8$ Å, $c = 48.5$ Å, $\beta = 102.6°$) and with all crystals of ligated CKS (*14*, *15*). X-ray data were collected on a rotating anode X-ray generator (Rigaku, model RU200B) with a multi-wire area detector (model X1000, Nicolet-Bruker) using Cu K_α radiation. The data were processed with program XDS (*16*) and scaled and merged with SCALA (*17*).

The CMP-Kdo complex was produced using a crystal of 400 × 160 × 80 μm^3 that was soaked for 90 min in 10 mM Kdo, 1.3 mM $MgCl_2$, 75 mM Tris-HCl, pH 9.4, 12% PEG-20000, and 150 mM $Ca(OAc)_2$. The soak was continued by applying 7 mM CTP, 7 mM Kdo, 1 mM $MgCl_2$, 80 mM Tris-HCl, pH 9.4, 13% PEG-20000, and 170 mM $Ca(OAc)_2$ for 15 min. The crystal was then transferred for about half a minute into 25% (v/v) glycerol, 15 mM Kdo, 75 mM Tris-HCl, 12% PEG-20000, and 150 mM $Ca(OAc)_2$, quickly frozen to 100 K and used for data collection. The crystal was isomorphous with those of unligated CKS and showed the cell parameters $a = 45.9$ Å, $b = 131.0$ Å, $c = 48.1$ Å, and $\beta = 102.3°$. It diffracted to 2.3 Å resolution. X-ray data were collected on a rotating anode X-ray generator (Rigaku model RU200B) using an image plate (MarResearch 30 cm) and processed with programs MOSFLM (*17*) and SCALA (*17*).

Table 1: X-ray Data Collection Statistics of Ligated CKS Crystals[a]

	CTP(100K)	CMP−Kdo
resolution range (Å)	29−2.6 (2.74−2.60)	33−2.6 (2.70−2.57)
unique reflections	14812 (1826)	15622 (2075)
multiplicity	1.8 (1.6)	5.9 (5.7)
R_{sym-I} (%)	6.8 (13)	11.5 (33)
average I/σ	9.9 (5.7)	6.0 (2.3)
completeness (%)	87 (74)	88 (81)

[a] All values in parentheses refer to the last shell. All data were collected at 100 K.

Table 2: Refinement Statistics of Ligated CKS Crystal Structures[a]

	CTP(100K)	CMP-Kdo
resolution	29−2.6	25−2.6
R_{cryst}	0.233	0.178
R_{free} (5% test set)	0.289	0.240
no. of atoms (average *B*-factors, Å^2)		
protein[b]	3740 (14)	3745 (26)
CMP-Kdo (subunit A)		36 (24)
CMP (subunit B)		21 (38)
CTP (subunit A)	29 (46)	
CTP (subunit B)	29 (21)	
solvent	190 (13)	267 (27)

[a] The root-mean-squares deviations of bond lengths and bond angles were in the ranges 0.007−0.010 Å and 1.3−1.4°, respectively. [b] Residues 242−245 of both subunits are missing in both structures, except for residue 242 in subunit A of the CMP-Kdo complex.

Structure Analyses. X-ray diffraction data of both complexes were measured to 2.6 Å resolution (Table 1). The structures were elucidated by difference Fourier techniques and subsequently refined by starting from the model of the unligated enzyme without water molecules (*14*, *15*). Both analyses began with a rigid body refinement (*18*). After that, we calculated an initial ($F_o - F_c$) map for locating the modifications. The models of the ligands CTP, CMP, and CMP-Kdo, respectively, were introduced into their structures using program O (*19*) and refined using the programs XPLOR (*18*) and CNS (*20*) with moderate noncrystallographic symmetry restraints between the polypeptides of the two subunits of the homodimer. Water molecules were introduced manually after the *R*-factor dropped below 27%. They were introduced wherever the ($F_o - F_c$) map showed density above 3 σ and the environment permitted hydrogen bonds. However, if the electron density of a water molecule dropped below 0.9 σ in the ($2F_o - F_c$) map, it was omitted from the model. The refinements finished with about 0.5 water molecules per residue as well as *R* and R_{free} values in an acceptable range (Table 2). For figure production we used the programs MOLSCRIPT (*21*) and Raster3D (*22*). The models of CTP, CMP, and CMP-Kdo were built using program SYBYL (Tripos Assoc., St. Louis/MO/USA).

RESULTS AND DISCUSSION

Structure Determination. CKS crystals contained a symmetric homodimer in the crystallographic asymmetric unit

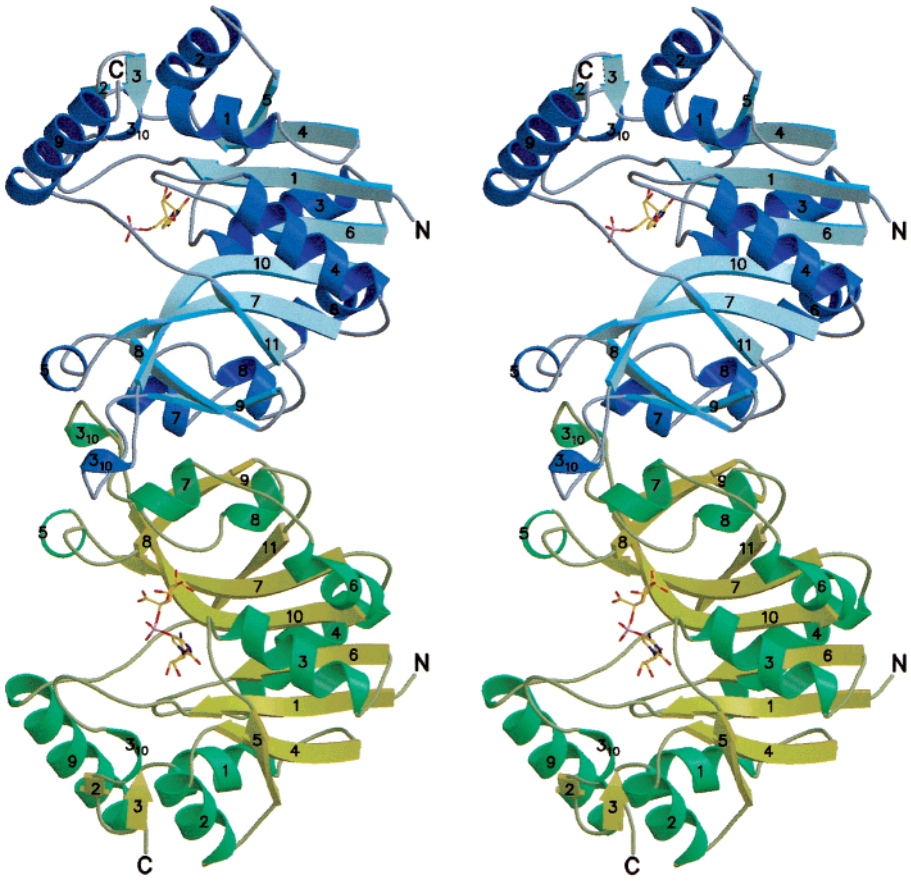

FIGURE 2: Stereo ribbon plot of CKS ligated with CMP-Kdo. The molecular 2-fold axis is noncrystallographic and lies horizontally in the paper plane. CMP-Kdo was produced in the crystal in subunit A (bottom) and conserved by freezing to 100 K. In subunit B (top), the soaked CTP was hydrolyzed to CMP.

and had a solvent content of 54% (*14*). Crystals of the CTP complex were produced by soaking and a subsequent quick freeze to 100 K. This complex was named "CTP(100K)" to distinguish it from the CTP complex established at room temperature (*15*) which differed in some essential details. The CMP-Kdo complex crystals were obtained by a reaction in the crystal that could be stopped at a high product occupancy by freezing quickly to 100 K. The crystals of both enzyme complexes were isomorphous to those of the unligated enzyme at room temperature, exhibiting cell axis differences of less than 2%. Despite numerous trials, Kdo alone could not be bound to the crystalline enzyme.

The refined final models of the CTP(100K)- and the CMP-Kdo complexes showed 89 and 93% of the mainchain dihedral angles of all nonglycine residues in the "most favored" regions and the remaining 11 and 7% in "additionally allowed" regions, respectively. Moreover, the side chain dihedral angles of Ile and Leu were concentrated in the allowed areas. The four C-terminal residues of both subunits remained essentially invisible in both 100 K structures, in contrast to the room-temperature structures where the four C-terminal residues of subunit A were rigidified by a crystal packing contact (*15*). A structural overview of the dimeric CMP-Kdo complex is given in Figure 2.

CTP(100K) Complex. After the quick freeze to 100 K, the soaked CKS crystals show the bound educt CTP in both subunits, though stronger and with lower *B*-factors in subunit B. This is in contrast to an earlier measurement at room temperature (*15*), where CTP was only bound to subunit B. The annealed ($F_o - F_c$) omit map of the more strongly bound CTP is shown in Figure 3. An even more interesting difference is observed with respect to the γ-phosphate. In the room temperature complex, this group and also the adjacent Arg15 pointed to the solvent. In the reported CTP-(100K) structure, however, the γ-phosphate is bound to the PP-loop including the side chain of Arg15, which has curled around. This applies to both subunits and most likely shows the true binding structure of CTP. The CTP(100K) complex does not contain the Mg^{2+} ion between the β- and γ-phosphates, which had been tentatively deduced from the room-temperature electron density map (*15*). The site in question is occupied by the γ-phosphate. The tentative Mg^{2+} at room temperature may have been a weak alternative site of the γ-phosphate.

The *B*-factor pattern of the CTP(100K) complex resembles that of the CTP complex at room temperature (*15*). In both cases the mobility of the PP-loop and of the adjacent loop around Asp225 is high in subunit A, while much lower in subunit B. Since CTP binds to both subunits of CTP(100K) in essentially the same manner, this mobility difference is probably caused by crystal contacts that vary between the two subunits being in different crystallographic environments (one dimer per asymmetric unit). Obviously, the more rigid site of subunit B facilitated nucleotide binding, as only this site accommodated ligands at room temperature (*15*).

CMP-Kdo Complex. The complex between CKS and the unstable product CMP-Kdo was obtained by soaking a CKS crystal with CTP, Kdo, and Mg^{2+}, and stopping the presumed

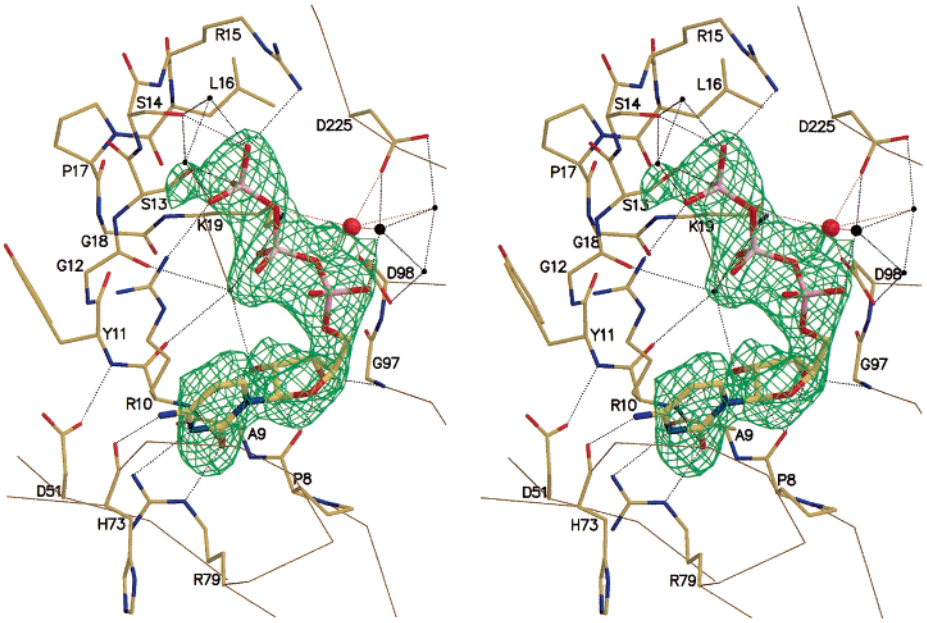

FIGURE 3: CTP bound to subunit B of CKS in the CTP(100K) complex, depicted together with the ($F_o - F_c$) electron density map at the 3 σ contour level. This map was obtained after removing the CTP model from the active center and annealing the remainder. The important residues are shown, they are embedded in their Cα chain traces. The putative Mg^{2+} is a red circle with red dotted lines extending to its contacting atoms. The average of the four short contact distances is 2.2 Å. Water molecules are black dots, the putative hydroxide being larger than the others. Hydrogen bonds are black dotted lines.

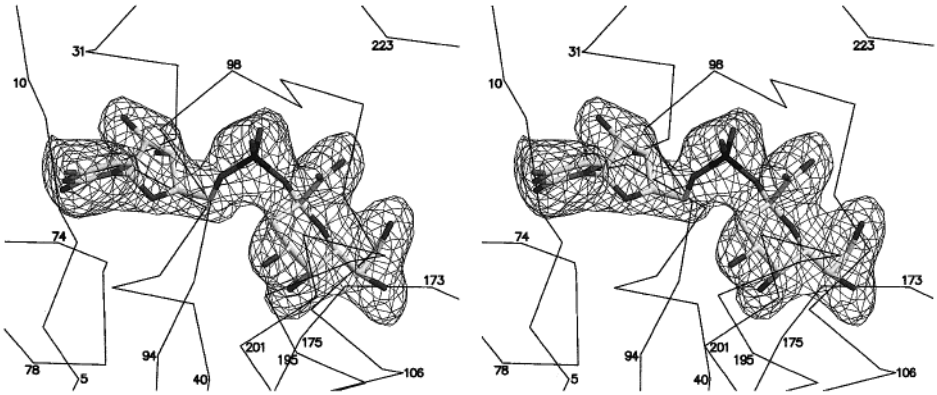

FIGURE 4: CMP-Kdo bound to CKS, which is represented by the surrounding Cα traces that carry some residue numbers. The depicted ($F_o - F_c$) electron density map was obtained after removing CMP-Kdo and annealing the remaining model. The contour level is at 3 σ. The density confirms the expected β-anomeric configuration and the $^5C_2$ chair conformation (Figure 1).

catalytic reaction by freezing to 100 K. As a result, the crystalline enzyme CKS produced CMP-Kdo in subunit A where the PP-loop and Asp225 are highly mobile, and it produced a CMP molecule in the more rigid subunit B (Figure 2). The observed CMP indicated that the applied CTP molecule had been hydrolyzed by an attacking water molecule substituting for Kdo. Both ligands were well-supported by electron density, the annealed ($F_o - F_c$) omit map of CMP-Kdo is depicted in Figure 4. The refinement resulted in a CMP-Kdo occupancy approaching 100%, which points to a surprisingly low off-rate of this catalytic product in the crystal. In any case, the observed product demonstrated that the crystalline CKS was active with respect to its more mobile subunit A, indicating that the observed structure represents the active enzyme.

The CMP moiety of CMP-Kdo is bound similarly as in the CTP(100K) complex. The Kdo moiety of CMP-Kdo uses its carboxyl and all four hydroxyl groups to bind to the protein, in addition to its nonpolar binding interactions with Val140 and Leu200. The 1-carboxylate forms a salt bridge to Arg155 and hydrogen bonds to well-connected water molecules. The 4-hydroxyl group binds to Glu201, the 5-hydroxyl to Glu201 and Tyr176, the 7-hydroxyl to His172 and Gln202, and the 8-hydroxyl to Wat10, which sits snugly between mainchain atoms.

When superimposing the subunit A chainfolds of the CMP-Kdo and the CTP(100 K) complexes, we observed a number of polypeptide displacements in the 1 to 2 Å range (Figure 5). This superposition was based on 96 C_α atoms of the polypeptide core with a root-mean-square deviation of 0.30 Å. It showed that the loops around residues 15, 51, 72, 138, 155, and 201 lining the active center cleft moved toward the reaction product CMP-Kdo and presumably clamped it down onto the protein. Moreover, it revealed a 1.5 Å displacement of the CMP moiety in the CTP(100K)- as compared to the CMP-Kdo complex, indicating a corresponding shift during the reaction. Since Kdo alone could not be bound to the crystalline enzyme, the Kdo shift during

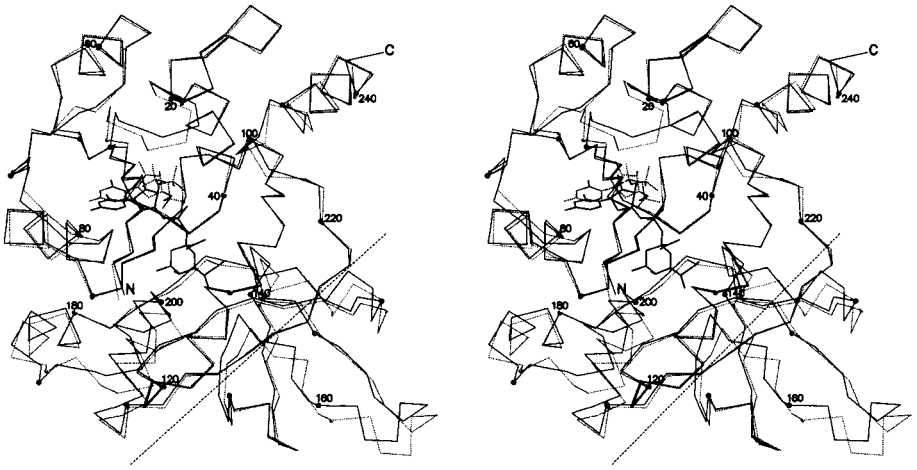

FIGURE 5: The induced fit during the production of CMP-Kdo demonstrated by a chainfold superposition of subunits A of the CTP(100K) (dotted lines) and the CMP-Kdo (solid lines) complexes. The superposition is based on 96 Cα atoms of the polypeptide core, namely, those at positions 2−9, 23−49, 66−70, 90−127, 175−182, and 210−219. The view is into the active center cleft, the width of which is reduced by about 3 Å.

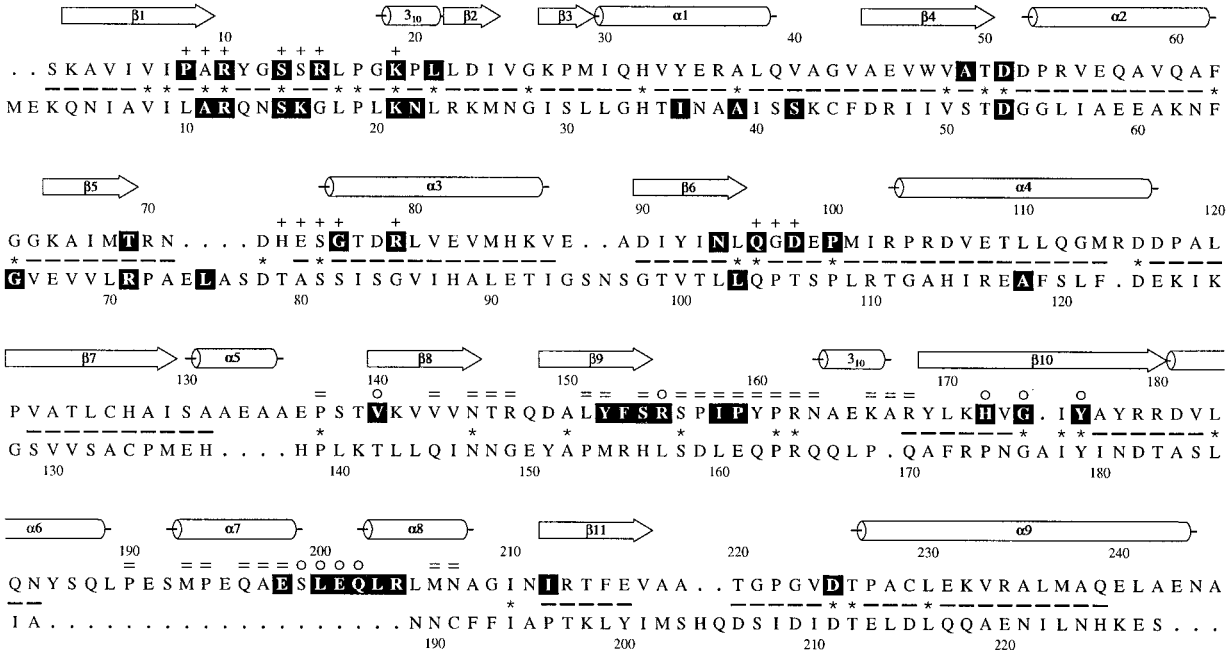

FIGURE 6: Structure-based sequence alignment of CKS (top line, the reported enzyme from *E. coli*) with CNS from *Neisseria meningitidis* (*25*) using Protein Data Bank file 1EYR (bottom line). The chain segments that superimposed within 3 Å are marked by (−) and the identical residues by (*). There are strong structural deviations at the dimer interface. The strictly conserved residues (*15*) within each of the two families are marked by black/white inversion. The secondary structure elements of CKS are given as a frame of reference. The CKS residues within 4 Å of CTP (+) and of Kdo (o) are labeled together with those at the dimer interface (=).

the induced fit cannot be quantified. The displacements of the Kdo-binding loops around 155 and 201 (Figure 5) suggest, however, that the Kdo shift is also around 1.5 Å.

Since CMP-Kdo has a half-life of about 30 min under physiological conditions (*23*, *24*), it has not yet been directly characterized and is not commercially available. The conformation of the displayed CMP-Kdo molecule in Figure 4 is therefore a novelty in itself. In contrast, the analogous activated sugar CMP-NeuAc produced by CMP-NeuAc synthetase (CNS, EC 2.7.7.43) has a half-life of several days (*23*, *24*) and is commercially available. We had used CMP-NeuAc for a soak at room temperature in an earlier analysis (*15*), observing that the CMP moiety was bound as usual to subunit B whereas the NeuAc moiety was rather disordered though localizable. In relation to the Kdo position of the true product CMP-Kdo, however, the NeuAc moiety was shifted across the protein surface with a sugar ring center displacement of 5 Å. Since Kdo fits conveniently and is supported by a well-developed density (Figure 4), there is no doubt that its location is correct.

Residue Conservation within the CKS Family. Sequence alignments of the reported CKS from *E. coli* with 12 other CKS sequences showed between 29 and 43% identical residues (*15*). The alignments revealed furthermore 33 strictly conserved positions, which are marked in Figure 6. Among them, six are at the CMP and eight at the Kdo moiety of CMP-Kdo. Three strictly conserved residues are at the β- and γ-phosphates of CTP, and a further five are at the interface, among them Pro159 with its *cis*-peptide bond. The observed ligand structures are therefore quite consistent with

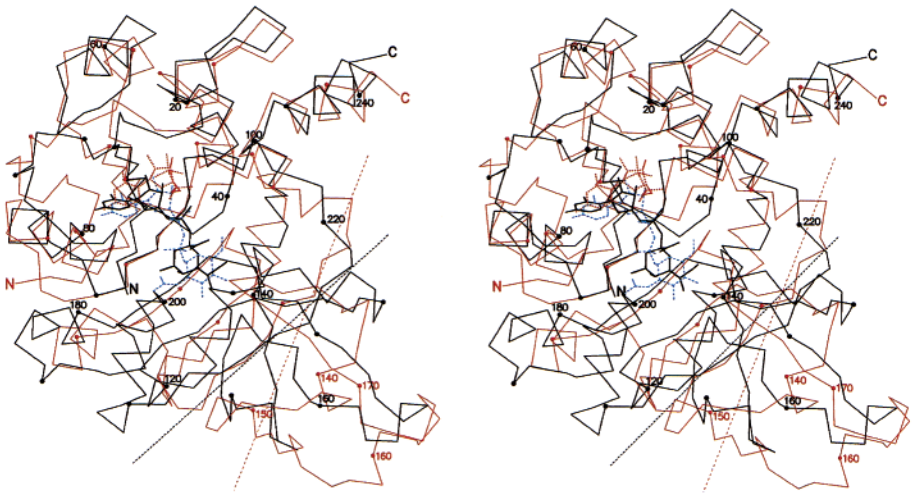

FIGURE 7: Stereoview of the superimposed Cα plots of CKS ligated with CMP-Kdo (black) and CNS ligated with CDP (red, ref. *25*). The 2-fold dimer axes are indicated. In a further superposition of the *N*-acetylglucosamine-1-phosphate uridyltransferase (*27*) with CKS, we display only the bound substrate UDP-*N*-acetylglucosamine (blue) as the chainfold comparison with CKS was shown earlier (*15*).

the conservation pattern. Moreover, this pattern was quite useful for the elucidation of the reaction mechanism. There are no further patches of strongly conserved residues anywhere at the surface so that we do not expect conserved interactions with yet unknown partner molecules.

Relationship to the CNS Family and to other Enzymes. The CKS and the CNS families of enzymes are exceptional in that they generate a sugar monophosphate and not the more common diphosphate diester. An earlier sequence-based alignment of 13 CKS family members with eight members of the CNS family demonstrated that the 100 N-terminal residues of all enzymes can be matched, revealing a clear evolutionary relationship (*15*). Now, the structure elucidation of CNS (*25*) allowed a more detailed comparison, showing that the similarity extends over the whole chain, except for a substantial deviation in the interface region. The chainfold homology is illustrated in Figure 7 and the corresponding peptide segments are marked in Figure 6. The strongest deviations are around positions 155 and 195 of CKS where numerous residues participate in the dimer interface and where Kdo is bound. The interface variations cause quite a different relative orientation of the two nucleotide-binding folds of CKS as compared with those of CNS. In relation to the nucleotide-binding fold itself, however, the observed CDP in CNS (*25*) is essentially at the same position as the CMP moiety of CMP-Kdo bound to CKS (Figure 7).

In their analysis, Mosimann et al. (*25*) suggested a binding location for NeuAc in CNS, which fits quite well the observed Kdo position in the CMP-Kdo complex with CKS. The reaction mechanism of both enzyme families appears to be similar because residues Arg10, Lys19, and Asp51 (CKS numbering) that are clearly involved in the reaction of CKS (*15*) are strictly conserved in both families (Figure 6). Moreover, the fourth strictly conserved residue in both families is Ser13, which binds the γ-phosphate of CTP (Figure 3).

Besides the rather close relationship between CKS and CNS, a more distant evolutionary connection exists to other enzymes processing nucleotide sugars. As can be deduced from the reported chainfold topologies (*14*, *26*), the core of the CKS chainfold is identical to the chainfold cores of the so-called "SGC superfamily" of enzymes that use nucleotide sugars either as an educt or as a product of the catalyzed reaction. Our knowledge about this superfamily has been enlarged appreciably through recent structure analyses (*27*−*40*). A superposition of one of these enzymes with CKS showed that the nucleotide and the sugar moieties bind at equivalent positions of the chainfold and deviate by less than 2 Å (Figure 7). CKS is therefore clearly a member of this superfamily. The same applies for CNS (*25*).

Reaction Mechanism. The nucleotide sugar CMP-Kdo is synthesized using Kdo, CTP, and Mg^{2+}. Under physiological conditions, Kdo is a mixture of pyranose and furanose forms, with only about 2% in the β-pyranose configuration (*41*) that is accepted by CKS (*42*). The pyranose ring of Kdo assumes the $^5C_2$ chair conformation (Figures 1 and 4) so that the β-anomeric hydroxyl group is equatorial (*43*). For catalysis the 2-hydroxyl group of Kdo should be backed up by a base that receives its proton, while its oxygen attacks the α-phosphorus atom of CTP. The required Mg^{2+} ion is commonly used for polarizing the attacked phosphorus atom.

When comparing all our CKS structures, we have to assume that displacements of up to 2 Å may occur during the reaction. Even with such shifts, however, there is no way of bringing a basic protein side chain to a suitable position to accept the proton from the 2-hydroxyl group of Kdo. We therefore conclude that the base should be a water molecule, as it was suggested for CNS (*25*). The position of this water molecule should be determined by the strictly conserved residues in this region, and these are Gln96, Asp98, and Asp225 (Figure 6) and possibly also by the 1-carboxylate of the substrate Kdo.

In Figure 8 the structures of the CTP(100K)- and CMP-Kdo complexes are superimposed on their polypeptide cores. The location of the 2-hydroxyl group of Kdo in the CMP-Kdo complex is most suitable for an attack at the α-phosphorus atom of the CTP(100K) complex. It is clear from Figure 8 that such an attack results in an S_N2 in-line reaction which inverts the α-phosphate to the conformation observed in CMP-Kdo. The leaving pyrophosphate is well-connected to the PP-loop, which is mobile and can move away. The strictly conserved Arg10, Arg15, and Lys19 are likely to neutralize the developing additional negative charge on the pyrophosphate. Consequently, the reaction geometry of CTP

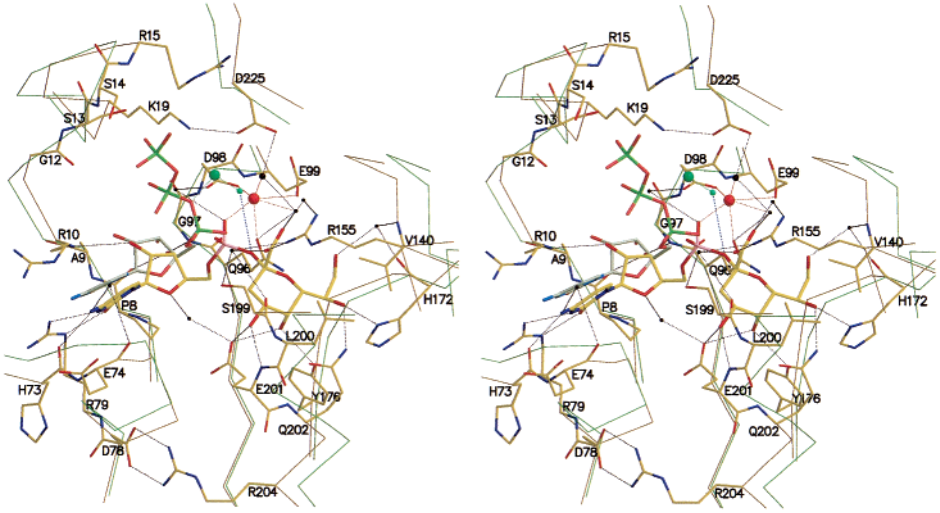

FIGURE 8: Stereoview of the detailed binding structure of CMP−Kdo to CKS. The important residues are embedded in their Cα chain traces (brown). The putative Mg^{2+} ion (peak height 3.9 σ in the final ($2F_o - F_c$) map) and the interactions with its ligands are red. Water molecules and hydrogen bonds are black. The putative hydroxide ion at a 2.3 Å distance to Mg^{2+} is somewhat enlarged. For reference, CTP and the putative Mg^{2+} (peak height 3.7 σ in the final ($2F_o - F_c$) map) with hydroxide and Cα traces of the CTP(100K) complex (all green) have been superimposed on the polypeptide cores (96 Cα atoms, see Figure 5). Mg^{2+} and hydroxide move by about 2 Å during the reaction. Presumably, the distance from the hydroxide of the CTP(100K) complex to the 2-oxygen of CMP-Kdo (blue, here 3.5 Å) is shortened during the reaction so that the hydroxide can pick up the proton.

and Kdo is clear, except for the locations of the Mg^{2+} and the required base.

Previously, we had suggested a Mg^{2+} position at the PP-loop in the room temperature complex with CTP because we observed a nearly octahedral ligand arrangement, although with rather long ligand distances (Figure 5 of ref *15*). Now we consider this proposed Mg^{2+} position obsolete because the CTP(100K) complex shows the γ-phosphate at this position which, in contrast to the room temperature structure, is further fastened by the strictly conserved Arg15. Furthermore, the CMP, CDP, and CTP complex structures at room temperature contained a peak with more density than a common water molecule and rather short distances to the α-phosphate as well as to Asp98 and Asp225. This peak lacked the expected octahedral ligand arrangement and was therefore considered a strongly bound water molecule (Figure 5 of ref *15*).

Now we find this peak again in both low-temperature complexes where it contacts Asp98 and the phosphate (Figure 8). Since the five shortest contact distances to this peak are below 2.5 Å and since the ligand spheres around this peak are consistent with octahedrons in both complexes, we assigned this peak now to a Mg^{2+} ion. In both complexes the putative Mg^{2+} ion is closely associated (average distance 2.1 Å) with a water molecule which we assume is a hydroxide ion (Figure 8). This hydroxide is at a position where it can act as a base during the nucleophilic attack of Kdo on CTP. It is hydrogen bonded to Asp225, to further water molecules and via one of them also to the 1-carboxylate of Kdo, which may therefore play a direct role in catalysis. It should be noted that, in the reverse reaction, the 1-carboxylate may facilitate the protonation of the bridging 2-oxygen of CMP-Kdo, explaining the short half-life of this compound in water.

These data suggest the reaction scheme sketched in Figure 9: CTP binds with its β- and γ-phosphates at the PP-loop and recruits Arg10, Ser13, Ser14, Arg15, and Lys19 as

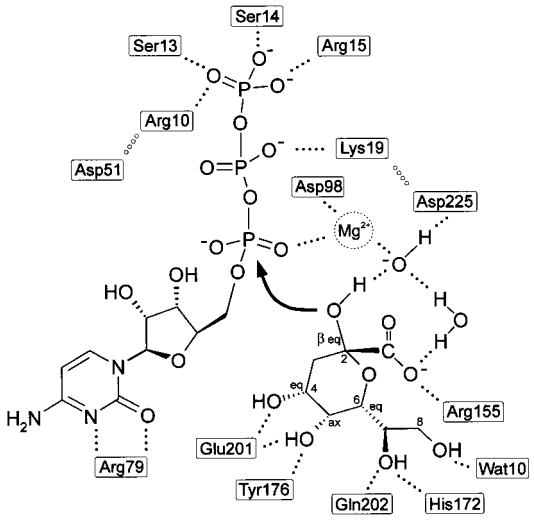

FIGURE 9: Proposed reaction mechanism of CKS. The β- and γ-phosphates of CTP are bound at the PP-loop. For pyrophosphate release Arg10 moves from the γ-phosphate away to Asp51, and Lys19 moves from the β-phosphate to Asp225. A putative Mg^{2+} ion between the α-phosphate, Asp98, and Asp225 binds a hydroxide ion (possibly a water molecule), which accepts the Kdo 2-hydroxyl proton during catalysis. The hydroxide is hydrogen bonded via a water molecule to the 1-carboxylate of Kdo. This indirect hydrogen bond may also occur when CMP-Kdo is dissolved in water, explaining its short half-life.

ligands (Figure 3). Mg^{2+} binds between the α-β-bridge oxygen of CTP, Asp98, and Asp225. Moreover, Mg^{2+} binds tightly to a hydroxide ion. On Kdo binding, Mg^{2+} and hydroxide shift toward Kdo so that Mg^{2+} polarizes the α-phosphorus atom and the hydroxide accepts the proton from the attacking 2-hydroxyl group of Kdo (Figure 8). After CMP-Kdo formation, Arg10 returns to its initial position where it forms a salt bridge with Asp51, and Lys19 moves to Asp225 so that the pyrophosphate can be released from the enzyme. The release of CMP-Kdo is probably much slower, as judged from its accumulation in the crystal. This pathway appears to be a reasonable working hypothesis,

although we had to postulate 2 Å shifts of the two mobile and transient participants Mg^{2+} and hydroxide.

ACKNOWLEDGMENT

We thank Dr. K. Jann for providing us with the gene of capsule-specific CKS from *E. coli*.

REFERENCES

1. Unger, F. M. (1981) *Adv. Carbohydr. Chem. Biochem. 38*, 323−388.
2. Raetz, C. R. H. (1990) *Annu. Rev. Biochem. 59*, 129−170.
3. Whitfield, C., and Valvano, M. A. (1993) *Adv. Microbial Physiol. 35*, 135−246.
4. Ray, P. H., Benedict, C. D., and Grasmuk, H. (1981) *J. Bacteriol. 145*, 1273−1280.
5. Goldman, R. C., Bolling, T. J., Kohlbrenner, W. E., Kim, Y., and Fox, J. L. (1986) *J. Biol. Chem. 261*, 15831−15835.
6. Gabriel, O. (1982) *Methods Enzymol. 83*, 332−353.
7. Finke, A., Roberts, I., Boulnois, G., Pazzani, C., and Jann, K. (1989) *J. Bacteriol. 171*, 3074−3079.
8. Jann, K., and Jann, B. (1992) *Can. J. Microbiol. 38*, 705−710.
9. Pazzani, C., Rosenow, C., Boulnois, G. J., Bronner, D., Jann, K., and Roberts, I. S. (1993) *J. Bacteriol.* 175, 5978−5983.
10. Rosenow, C., Roberts, I. S., and Jann, K. (1995) *FEMS Microbiol. Lett. 125*, 159−164.
11. Cooke, E. M. (1985) *J. Hygiene 95*, 523−530.
12. Hoffman, J. A., Wass, C., Stins, M. F., and Kim, K. S. (1999) *Infect., Immun. 67*, 3566−3570.
13. Hammond, S. M., Claesson, A., Jansson, A. M., Larsson, L.-G., Pring, B. G., Town, C. M., and Ekström, B. (1987) *Nature 327*, 730−732.
14. Jelakovic, S., Jann, K., and Schulz, G. E. (1996) *FEBS Lett. 391*, 157−161.
15. Jelakovic, S., and Schulz, G. E. (2001) *J. Mol. Biol. 312*, 143−155.
16. Kabsch, W. (1988) *J. Appl. Crystallogr. 21*, 916−924.
17. CCP4, Collaborative Computing Project, No. 4 (1994) *Acta Crystallogr. Sect. D 50*, 760−763.
18. Brünger, A. T. (1992) X-PLOR Version 3.1. A system for X-ray crystallography and NMR. Yale University Press, New Haven.
19. Jones, T. A., Zou, J.-Y., Cowan, S. W., and Kjeldgaard, M. (1991) *Acta Crystallog. Sect. A 47*, 110−119.
20. Brünger, A. T., Adams, P. D., Clore, G. M., DeLano, W. L., Gros, P., Grosse-Kunstleve, R. W., Jiang, J.-S., Kuszewski, J., Nilges, M., Pannu, N. S., Read, R. J., Rice, L. M., Simonson, T., and Warren, G. L. (1998) *Acta Crystallog. Sect. D 54*, 905−921.
21. Kraulis, P. J. (1991) *J. Appl. Crystallog. 24*, 946−950.
22. Merritt, E. A., and Bacon, D. J. (1997) *Methods Enzymol. 277*, 505−524.
23. Sugai, T., Lin, C.-H., Shen, G.-J., and Wong C.-H. (1995) *Bioorg. Med. Chem. 3*, 313−320.
24. Lin, C.-H., Murray, B. W., Ollmann, I. R., and Wong, C.-H. (1997). *Biochemistry 36*, 780−785.
25. Mosimann, S. C., Gilbert, M., Dombroswki, D., To, R., Wakarchuk, W., and Strynadka, N. C. J. (2001) *J. Biol. Chem. 276*, 8190−8196.
26. Ünligil, U. M., Zhou, S., Yuwaraj, S., Sarkar, M., Schachter, H., and Rini, J. M. (2000) *EMBO J. 19*, 5269−5280.
27. Brown, K., Pompeo, F., Dixon, S., Mengin-Lecreulx, D., Cambillau, C., and Bourne, Y. (1999) *EMBO J. 18*, 4096−4107.
28. Charnock, S. J., and Davies, G. J. (1999) *Biochemistry 38*, 6380−6385.
29. Gastinel, L. N., Cambillau, C., and Bourne, Y. (1999) *EMBO J. 18*, 3546−3557.
30. Blankenfeldt, W., Asuncion, M., Lam, J. S., and Naismith, J. H. (2000) *EMBO J. 19*, 6652−6663.
31. Kostrewa, D., D'Arcy, A., Takacs, B., and Kamber, M. (2001) *J. Mol. Biol. 305*, 279−289.
32. Olsen, L. R., and Roderick, S. L. (2001) *Biochemistry 40*, 1913−1921.
33. Barton, W. A., Lesniak, J., Biggins, J. B., Jeffrey, P. D., Jiang, J., Rajashankar, K. R., Thorson, J. S., and Nikolov, D. B. (2001) *Nat. Struct. Biol. 6*, 545−551.
34. Stevenson, C. E. M., Sargent, F., Buchanan, G., Palmer, T., and Lawson, D. M. (2000) *Structure 8*, 1115−1125.
35. Pedersen, L. C., Tsuchida, K., Kitagawa, H., Sugahara, K., Darden, T. A., and Negishi, M. (2000) *J. Biol. Chem. 275*, 34580−34585.
36. Lake, M. W., Temple, C. A., Rajagopalan, K. V., and Schindelin, H. (2000) *J. Biol. Chem. 275*, 40211−40217.
37. Persson, K., Ly, H. D., Dieckelmann, M., Wakarchuk, W. W., Withers, S. G., and Strynadka, N. C. J. (2001) *Nat. Struct. Biol. 8*, 166−175.
38. Richard, S. B., Bowman, M. E., Kwiatkowski, W., Kang, I., Chow, C., Lillo, A. M., Cane, D. E., and Noel, J. P. (2001) *Nat. Struct. Biol. 8*, 641−648.
39. Gastinel, L. N., Bignon, C., Misra, A. K., Hindsgaul, O., Shaper, J. H., and Joziasse, D. H. (2001) *EMBO J. 20*, 638−649.
40. Sulzenbacher, G., Gal, L., Peneff, C., Fassy, F., and Bourne, Y. (2001) *J. Biol. Chem. 276*, 11844−11851.
41. Brade, H., Zähringer, U., Rietschel, E. T., Christian, R., Schulz, G., and Unger, F. M. (1984) *Carbohydr. Res. 134*, 157−166.
42. Kohlbrenner, W. E., and Fesik, S. W. (1985) *J. Biol. Chem. 260*, 14695−14700.
43. Birnbaum, G. I., Roy, R., Brisson, J.-R., and Jennings, H. J. (1987) *J. Carbohydr. Chem. 6*, 17−39.

BI0119060